AIAA 79-1738R

Control of Large Flexible Space Structures Using Pole Placement Design Techniques

Y. W. Wu* and R. B. Rice†
Martin Marietta Corp., Denver, Colo.
and
J. N. Juang‡
Jet Propulsion Laboratory, California Institute of Technology, Pasadena, Calif.

A design approach using pole placement techniques for a class of large flexible space structures is developed. The numerical problems of the pole placement algorithm when used on large-dimensional systems having extremely low-frequency eigenvalues are examined. It is shown that these numerical difficulties may be overcome by properly selecting the sensor/actuator locations and introducing a frequency scaling scheme. The concepts presented are illustrated by computer simulations of the linear feedback control design for a representative large spacecraft consisting of a small rigid core with 10 radial booms (five booms 1000 ft long and five shorter booms 700 ft long) lying in a plane.

Introduction

THE attitude control of space structures having very large dimensions, low rigidity, and light damping has attracted increasing attention during recent years.[1-6] The resulting system model describing the structure is usually of large dimension, cross-coupled between planes, and has characteristic structural roots of extremely low frequency.

To model a highly flexible large space structure, a large number of vibration modes are needed to describe the dynamic behavior; however, due to the limitations of onboard computer capacity, it is only possible to consider several critical modes to be controlled out of many significant modes. Numerous technical articles[7-9] address the problems of choosing the controlled modes. Spillover problems created by this truncation are considered in Ref. 10. The minimum sensor/actuator requirement for controlling the system can be determined from the concepts of controllability and observability as shown in Refs. 11 and 12.

For attitude control, when the system bandwidth becomes large enough to approach or overlap some of the bending mode frequencies, these may no longer be ignored in the synthesis. Similarly, for precise pointing control, the number of modes beside the rigid-body modes to be controlled will significantly increase. A multiple-sensor/actuator type controller is required to deal with such large space structure systems. For these systems, classical single control loop design practices become inadequate because a designer has difficulty coping with more than three or four control parameters at once, especially when frequency separation approximations become impractical. On the other hand, modern control techniques can directly provide the multiloop control gains to obtain the required system performance.

In this paper, the focus is on control of large space structures that employ pole placement techniques. The numerical difficulties of the approach are also examined. Although the theory and associated algorithms using pole placement have been well developed,[13-16] few investigators have addressed the numerical problems that arise from large-dimension systems and the extremely low-frequency eigenvalues that occur in large space structure models. The following will show that the large dimensionality problem can be overcome by properly selecting the sensor/actuator locations, such that the controlled system may be partitioned into several weakly coupled subsystems; the subcontroller gains may be obtained based on these reduced-order systems. The numerical problem can usually be overcome by introducing a frequency scaling technique. The philosophy of this method is to rescale by the proper transformation so that the mode frequencies are no longer close to zero.

Presented as Paper 79-1738 at the AIAA Guidance and Control Conference, Boulder, Colo., Aug. 6-8, 1979; submitted Oct. 23, 1979; revision received Aug. 11, 1980.

*Staff Engineer, Guidance and Control Section; currently with Hughes Aircraft Company, Culver City, Calif. Member AIAA.
†Staff Engineer, Guidance and Control Section. Member AIAA.
‡Member of the Technical Staff, Automated System Section, Control and Energy Conversion Division. Member AIAA.

System Model and Control Design

Consider the class of flexible systems with N controlled modes described by

$$\ddot{u}_i + 2\zeta_i\omega_i\dot{u}_i + \omega_i^2 u_i = \sum_{j=1}^{L} b_{ij} f_j \tag{1}$$

where $u_i(t)$ represents the ith mode amplitudes with damping ratios ζ_i, mode frequencies ω_i, and the jth point force actuators f_j. The M sensors are described by

$$y_k = \sum_{i=1}^{N} c_{ik} u_i + d_{ik}\dot{u}_i \tag{2}$$

Equations (1) and (2) can be rewritten into the following state equation form:

$$\dot{x} = Ax + Bf \tag{3}$$

$$y = Cx \tag{4}$$

by introducing

$$x = [u_1, \dot{u}_1, \ldots, u_{NI}, \dot{u}_{NI} \mid \omega_{NI+1}u_{NI+1}, \dot{u}_{NI+1}, \ldots, \omega_N u_N, \dot{u}_N]^T$$

$$y = [y_1 y_2, \ldots, y_M]^T \qquad f = [f_1 f_2, \ldots, f_L]^T \tag{5}$$

where

$$A = \text{diag}[A_1 A_2, \ldots, A_N]$$

$$A_i = \begin{bmatrix} 0 & 1 \\ 0 & 0 \end{bmatrix} \qquad (i = 1,2, \ldots, N_I)$$

$$A_i = \begin{bmatrix} 0 & \omega_i \\ -\omega_i & -2\zeta_i\omega_i \end{bmatrix} \qquad (i=N_I+1, \ldots, N) \tag{6}$$

Modes 1 through N_I indicate the rigid-body modes, the rest are flexible modes.

It is assumed that a sufficient number of sensors and actuators are selected and properly located such that (A,B,C) is controllable and observable.

The theory and associated algorithms for stabilizing the system [Eqs. (3) and (4)] either by using pole placement or minimizing the chosen quadratic cost function[17,18] have been well developed. This paper examines a design approach that uses the pole placement techniques, which allow a designer to have direct control over the closed-loop system eigenvalues.

There are several algorithms that have been developed for pole placement. Among them, the Simon-Mitter (SM) algorithm[13,14] and transformation algorithm[15,16] are the most popular. The SM algorithm was developed based on classical control theory and is easy to interpret in the Laplace domain. However, the SM algorithm, in general, requires complex variable calculations; that is, complex eigenvectors, complex residues, complex matrix inversion, etc. This inherently increases the computation accuracy requirements. On the other hand, the transformation algorithm only uses real transformation and avoids complex variable calculations, as follows.

Two matrix inversions are required in the algorithm, the controllability matrix of (A,B) and $(A+BK_i,b_i)$ where b_i is the ith column of matrix B, and K_i is the matrix that transfers a noncyclic matrix A into a cyclic matrix $A+BK_i$. Both controllability matrices may be nearly singular as a result of large dimensions and extremely low frequencies in matrix A. These two factors will affect the numerical accuracy during the pole placement process.

By taking advantage of weak coupling between planes, the dimensionality problem may be overcome by properly selecting sensor/actuator locations so that the original system [Eqs. (3) and (4)] can be partitioned into k interconnected subsystems

$$\begin{bmatrix} \dot{X}_1 \\ \dot{X}_2 \\ \cdot \\ \cdot \\ \cdot \\ \dot{X}_k \end{bmatrix} = \begin{bmatrix} A_1 & & & 0 \\ & A_2 & & \\ & & \cdot & \\ & & & A_k \end{bmatrix} \begin{bmatrix} X_1 \\ X_2 \\ \cdot \\ \cdot \\ \cdot \\ X_k \end{bmatrix} \begin{bmatrix} B_{11} & B_{12} & \ldots & B_{1k} \\ 0 & B_{22} & \ldots & B_{2k} \\ \cdot & & & \\ \cdot & & & \\ \cdot & & & \\ 0 & 0 & \ldots & B_{kk} \end{bmatrix} \begin{bmatrix} u_1 \\ u_2 \\ \cdot \\ \cdot \\ \cdot \\ u_k \end{bmatrix} \tag{7}$$

$$Y = \begin{bmatrix} Y_1 \\ Y_2 \\ \cdot \\ \cdot \\ \cdot \\ Y_k \end{bmatrix} = \begin{bmatrix} C_{11} & 0 & \ldots & 0 \\ C_{21} & C_{22} & \ldots & 0 \\ \cdot & & & \cdot \\ \cdot & & & \cdot \\ \cdot & & & \cdot \\ C_{k1} & C_{k2} & \ldots & C_{kk} \end{bmatrix} \begin{bmatrix} X_1 \\ X_2 \\ \cdot \\ \cdot \\ \cdot \\ X_k \end{bmatrix} \tag{8}$$

The controllers u_i using local feedback are then easily designed provided all the subsystems are controllable and observable. To preserve the stability of the composite system by using only local feedback, state estimate feedback must be used instead of direct output feedback. This can be easily shown, without loss of generality, by considering two subsystems:

$$\begin{bmatrix} \dot{X}_1 \\ \dot{X}_2 \end{bmatrix} = \begin{bmatrix} \bar{A}_1 & 0 \\ 0 & \bar{A}_2 \end{bmatrix} \begin{bmatrix} X_1 \\ X_2 \end{bmatrix} + \begin{bmatrix} B_{11} & B_{12} \\ 0 & B_{22} \end{bmatrix} \begin{bmatrix} u_1 \\ u_2 \end{bmatrix} \tag{9}$$

$$Y = \begin{bmatrix} C_{11} & 0 \\ C_{21} & C_{22} \end{bmatrix} \begin{bmatrix} X_1 \\ X_2 \end{bmatrix} \tag{10}$$

For the case with local state estimate feedback,

$$u_1 = k_1\hat{X}_1 \qquad u_2 = k_2\hat{X}_2 \tag{11}$$

where

$$\dot{\hat{X}}_2 = \bar{A}_2\hat{X}_2 + B_{22}u_2 + K_{C2}[Y_2 - C_{21}\hat{X}_1 - C_{22}\hat{X}_2] \tag{12}$$

$$\dot{\hat{X}}_1 = \bar{A}_1\hat{X}_1 + B_{11}u_1 + B_{12}u_2 + K_{C1}[Y_1 - C_{11}\hat{X}_1] \tag{13}$$

and defining

$$e_1 = X_1 - \hat{X}_1 \qquad e_2 = X_2 - \hat{X}_2 \tag{14}$$

the composite system is then

$$\begin{bmatrix} \dot{\hat{X}}_1 \\ \dot{\hat{X}}_2 \\ \dot{e}_1 \\ \dot{e}_2 \end{bmatrix} = \left[\begin{array}{cc:cc} \bar{A}_1+B_{11}K_1 & B_{12}K_2 & K_{C1}C_{11} & 0 \\ 0 & \bar{A}_2+B_{22}K_2 & K_{C2}C_{21} & K_{C2}C_{22} \\ \hdashline 0 & 0 & \bar{A}_1-K_{C1}C_{11} & 0 \\ 0 & 0 & K_{C2}C_{21} & \bar{A}_2-K_{C2}C_{22} \end{array}\right] \begin{bmatrix} X_1 \\ X_2 \\ e_1 \\ e_2 \end{bmatrix} \tag{15}$$

which is stable, provided that (K_1,K_2,K_{C1},K_{C2}) are chosen such that $(\bar{A}_1+B_{11}K_1)$, $(\bar{A}_2+B_{22}K_2)$, $(\bar{A}_1-K_{C1}C_{11})$, and $(\bar{A}_2-K_{C2}C_{22})$ all have eigenvalues with negative real parts.

For the case with local output feedback,

$$u_1=H_1Y_1 \qquad u_2=H_2Y_2 \tag{16}$$

and the composite system is

$$\begin{bmatrix} \dot{X}_1 \\ \dot{X}_2 \end{bmatrix} = \begin{bmatrix} \bar{A}_1+B_{11}H_1C_{11} & B_{12}H_2C_{22} \\ +B_{12}H_2C_{21} & \\ B_{22}H_2C_{21} & \bar{A}_2+B_{22}H_2C_{22} \end{bmatrix} \begin{bmatrix} X_1 \\ X_2 \end{bmatrix} \tag{17}$$

which can be unstable even if matrices $(\bar{A}_1+B_{11}H_1C_{11})$, $(\bar{A}_2+B_{22}H_2C_{22})$ have stable eigenvalues. This leads to the following results:

Theorem 1: Suppose the system [Eqs. (3) and (4)] can be decomposed into k interconnected subsystems [Eqs. (7) and (8)], and $(\bar{A}_i,B_{ii},C_{ii})$ are controllable and observable for all i, then the composite systems can be stabilized by local state estimate feedback.

Frequency Scaling

Numerical difficulty usually occurs when applying pole placement methods to systems whose modes are extremely low frequency and have light damping (0.005). This problem can usually be improved by introducing a frequency scaling technique that essentially moves all the low frequencies away from zero. This allows the generation of feedback gains in the new coordinate system and avoids the numerical difficulty. Once the feedback gain constants are found in the new coordinate system, one can transfer back to the original system to obtain the desired feedback gain constants.

There exists many transformation functions that one can use to effectively increase the frequencies. In the following, a simple scaling scheme is introduced such that the desired gains can be easily calculated in terms of gains obtained in the time-scaled system.

Let the original system be described by

$$\dot{x}(t)=Ax(t)+Bf(t) \tag{18}$$

Define a scaling factor α by

$$t'=\alpha t \tag{19}$$

Furthermore, let

$$V_i(t') \triangleq u_i(t)\,|_{t=t'/\alpha} \tag{20}$$

and

$$\bar{f}_i(t')=(1/\alpha^2)f_i(t)\,|_{t=t'/\alpha} \tag{21}$$

Then the new coordinate system associated with $V_i(t)$ can be written as

$$\dot{Y}(t')=\bar{A}Y(t')+\bar{B}\bar{f}(t') \tag{22}$$

where

$$Y(t')=[V_1(t'),\dot{V}_1(t')\ldots V_{N1}(t'),\dot{V}_{N1}(t'),$$
$$\omega'_{N1+1}V_{N1+1}(t'),\dot{V}_{N1+1}(t')\ldots\omega'_NV_N(t),\dot{V}_N(t)]$$

It can be easily verified that the matrix $\bar{A}$ has the following form:

$$\bar{A}=\text{diag}[\bar{A}_1\bar{A}_2\ldots\bar{A}_N]$$

$$\bar{A}_i=\begin{bmatrix} 0 & 1 \\ 0 & 0 \end{bmatrix} \qquad (i=1,2,\ldots,N_1)$$

$$\bar{A}_i=\begin{bmatrix} 0 & \omega'_i \\ -\omega'_i & -2\zeta_i\omega'_i \end{bmatrix} \qquad (i=N_1+1,\ldots,N) \tag{23}$$

where

$$\omega'_i=\omega_i/\alpha$$

Hence, the open-loop eigenvalues of the new coordinate system have effectively been increased $1/\alpha$ times if α is chosen to be a small, positive real value.

Theorem 2: Let

$$f(t)=Kx(t) \qquad \bar{f}(t')=\bar{K}\bar{Y}(t') \qquad \bar{B}=B \tag{24}$$

Then,

$$\lambda_i(A+BK)=\alpha\bar{\lambda}_i(\bar{A}+\bar{B}\bar{K})$$

and

$$k^i_{1j}=\overline{\alpha k}^i_{1j} \qquad \text{for} \quad \omega_j\neq 0$$
$$k^i_{1j}=\alpha^2\bar{k}^i_{1j} \qquad \text{for} \quad \omega_j=0$$
$$k^i_{2j}=\alpha\bar{k}^i_{2j} \qquad \text{for all } \omega_j$$

where K^i_{1j} are the coefficients associated with the displacement feedback and K^i_{2j} are the coefficients associated with velocity feedback.

Proof: Because

$$u_i(t)=V_i(t')\,|_{t'=\alpha t}$$

Taking the Laplace transform gives

$$\mathcal{L}\{u_i(t)\}=\mathcal{L}\{V_i(\alpha t)\}=V_i(S')\,|_{S'=S/\alpha}$$

$$=\frac{\bar{N}_i(S')}{\bar{D}_i(S')}\Big|_{S'=S/\alpha}=\frac{\bar{N}_i(S')}{\prod_i(S'-\lambda_i)}\Big|_{S'=S/\alpha}$$

or

$$\bar{D}_i(S)=\prod_i(S-\lambda_i)=\prod_i(S-\alpha\bar{\lambda}_i)$$

which implies

$$\lambda_i = \alpha\bar{\lambda}_i \qquad \text{for all } i$$

Furthermore, Eqs. (21) and (24) give

$$f_i(t) = \alpha^2 \bar{f}_i(t')\,|_{t'=\alpha t}$$

$$= \alpha^2\left[\sum_{j=1}^{N_1} \bar{k}^i_{1j} V_j(t') + \sum_{j=N_1+1}^{N} \bar{k}^i_{1j}\omega'_j V_j(t') + \sum_{j=1}^{N} \bar{k}^i_{2j}\dot{V}_j(t')\right]$$

$$= \alpha^2\left[\sum_{j=1}^{N_1} \bar{k}^i_{1j} u_j(t) + \sum_{j=N_1+1}^{N} \bar{k}^i_{1j}\left(\frac{\omega_j}{\alpha}\right)u_j(t)\right]$$

$$+ \alpha^2\left[\sum_{j=1}^{N} \frac{\bar{k}^i_{2j}}{\alpha}\dot{u}_j(t)\right] = \left[\sum_{j=1}^{N_1} (\alpha^2 \bar{k}^i_{1j})\, u_j(t)\right.$$

$$\left. + \sum_{j=N_1+1}^{N} (\alpha\bar{k}^i_{1j})\,(\omega_j u_j(t)) + \sum_{j=1}^{N} (\alpha\bar{k}^i_{2j})\,\dot{u}_j(t)\right]$$

Example and Design Results

To demonstrate this design approach, a representative spacecraft is considered consisting of a small rigid core with ten radial booms lying in a plane as shown in Fig. 1. There are five booms 1000 ft long and five shorter booms 700 ft long. Each boom is modeled by five nodes, each with four lateral degrees-of-freedom (DOF). The first 26 modes, as listed in Table 1, are selected for linear control design. Two types of actuators are used—momentum wheels and thrusters—to generate the input matrix B. In addition, two types of sensors are used—angular and displacement sensors—to generate the output matrix C.

To avoid large dimensions, the location and type of sensors and actuators were made such that the total system could be partitioned into four subsystems with weak intercoupling as follows:

$$\begin{bmatrix}\dot{X}_1\\ \dot{X}_2\\ \dot{X}_3\\ \dot{X}_4\end{bmatrix} = \begin{bmatrix}A_1 & 0 & 0 & 0\\ 0 & A_2 & 0 & 0\\ 0 & 0 & A_3 & 0\\ 0 & 0 & 0 & A_4\end{bmatrix}\begin{bmatrix}X_1\\ X_2\\ X_3\\ X_4\end{bmatrix}$$

$$+ \begin{bmatrix}B_{11} & B_{12} & B_{13} & B_{14}\\ 0 & B_{22} & B_{23} & B_{24}\\ 0 & 0 & B_{33} & 0\\ 0 & 0 & 0 & B_{24}\end{bmatrix}\begin{bmatrix}u_1\\ u_2\\ u_3\\ u_4\end{bmatrix}$$

$$Y = \begin{bmatrix}C_{11} & 0 & 0 & 0\\ C_{12} & C_{22} & 0 & 0\\ C_{13} & C_{23} & C_{33} & 0\\ C_{14} & C_{24} & 0 & C_{44}\end{bmatrix}\begin{bmatrix}X_1\\ X_2\\ X_3\\ X_4\end{bmatrix}$$

Here X_1 represents the 3-DOF rotation motion of the rigid body plus six coupled rotational modes; X_2 represents the 3-DOF translation motion of the rigid body plus six coupled translational modes; and X_3 represents the four natural modes (modes 7-10) associated with the long booms. Three pairs of sensors and actuators (angular sensors and moment generators) located in the hub were selected to control X_1, one pair pointing in the direction of boom 3, one pair pointing in the direction of boom 5, and the third pair pointing in the Z direction (Fig. 2). Similarly, three pairs of sensors and actuators (displacement sensors and thrusters) were located in the hub, as shown in Fig. 2, to control X_2. One pair points in the direction of boom 2, one pair in the direction of boom 4, and the third pair in the Z direction. To control X_3, X_4, another eight pairs of sensors/actuators located on the booms, two-fifths away from the hub, were selected as shown in Fig. 3.

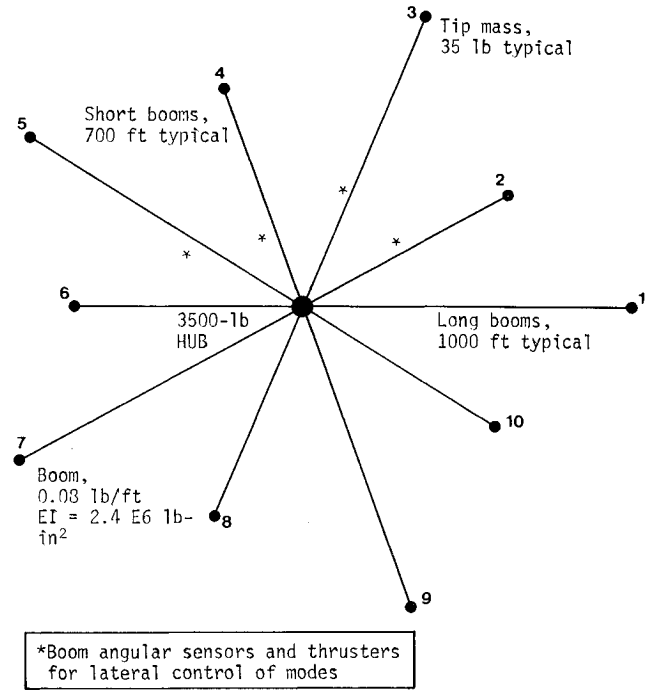

Fig. 1 Vehicle configuration, plan view.

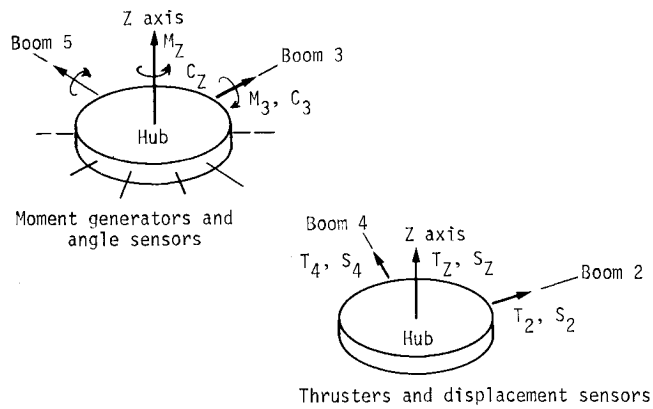

Fig. 2 Sensor and actuator placement for control of rigid-body and modes 11-16 plus modes 21-26 (arrow indicates sensitive axis).

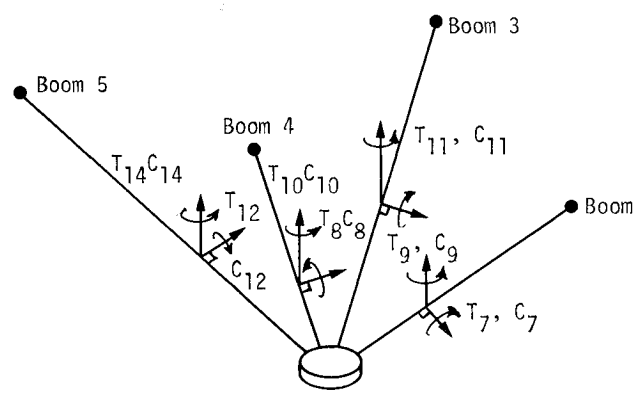

Fig. 3 Angle sensor and thruster placement for control of modes 7-10 and modes 17-20 (located at 2/5 of length).

Table 1 First 26-mode frequencies

Mode number	ω_i^2 rad^2/s^2	Identification
1	0	X
2	0	Y rigid-body
3	0	Z
4	0	θx
5	0	θy
6	0	θz
7	2.97871×10^{-5}	Natural modes
8	2.97871×10^{-5}	Long booms
9	2.97871×10^{-5}	
10	2.97871×10^{-5}	
11	3.15720×10^{-5}	X rigid-body
12	3.15720×10^{-5}	Y &
13	3.34738×10^{-5}	Z long booms
14	5.74280×10^{-5}	θx
15	5.74280×10^{-5}	θy
16	5.74280×10^{-5}	θz
17	9.71707×10^{-5}	Natural modes
18	9.71707×10^{-5}	Short booms
19	9.71707×10^{-5}	
20	9.71707×10^{-5}	
21	1.02512×10^{-4}	X
22	1.02512×10^{-4}	Y long & short & RB
23	1.02512×10^{-4}	Z
24	2.57868×10^{-3}	θx
25	2.57868×10^{-3}	θy
26	2.58809×10^{-3}	θz

Frequency scaling is applied here to find the gain constants K_1, K_2. In this example, α is 0.01. Full state estimates for each subsystem are generated for feedback control. The estimator poles are located further to the left of the closed-loop poles λ_i. This produces an estimator that is faster than the system it is controlling. The desired closed-loop pole locations of this example are chosen such that the damping ratios of rigid body modes are approximately equal to 0.55 and the damping ratio of all the deflection modes is increased from 0.005 to approximately 0.1. Tables 2 and 3 summarize the design results.

Comments

1) The frequency scaling of $\alpha = 0.01$ yields stable numerical results. It was found that the magnitude of the gain constants K_1, K_2 depends on the scaling factor α. The relation between the scaling factor and gain constants K is yet unclear, although simulations showed the magnitude of the gain constants K tends to be smaller as α becomes smaller.

2) In theory, one can control all 26 modes of this structure by using only eight actuators and eight sensors. Unfortunately, the open-loop system has 12 zero rigid-body eigenvalues plus extremely small eigenvalues near zero, which creates numerical difficulties for the pole placement algorithm. In practice, the system is almost uncontrollable. This indicates the minimal number of sensors/actuators may not be practical to control all modes.

Table 2 Control gain constants

K_1			K_2		
$u_{\theta xy}$	$u_{\theta xy}$	$u_{\theta z}$	u_{xy}	u_{xy}	u_z
-2.982×10	1.508×10^{-2}	0.0	1.065×10^{-2}	-2.707×10^{-3}	0.0
-2.409×10^{2}	-2.287×10^{-2}	0.0	1.814	7.490×10^{-3}	0.0
1.877×10	-1.096×10^{-2}	0.0	7.230×10^{-3}	-1.966×10^{-3}	0.0
-6.492×10^{2}	1.662×10^{-2}	0.0	1.153	5.440×10^{-3}	0.0
0.0	0.0	-2.355×10^{-1}	0.0	0.0	-1.036×10^{-3}
0.0	0.0	-3.104×10	0.0	0.0	-1.568×10^{-2}
3.498×10^{3}	-1.809	0.0	-4.818	2.893	0.0
-2.149×10	2.044×10^{-2}	0.0	-7.057	-4.048×10^{-2}	0.0
-6.934×10^{3}	3.611	0.0	-3.130	1.938	0.0
5.007×10	-4.080×10^{-2}	0.0	-4.575	-2.630×10^{-2}	0.0
0.0	0.0	8.511	0.0	0.0	6.487×10^{-2}
0.0	0.0	4.901×10^{-1}	0.0	0.0	-6.303×10^{-2}
9.355×10^{3}	-1.183×10^{-3}	0.0	-9.520×10^{-4}	-5.078×10^{-1}	0.0
-9.539×10^{2}	2.213×10^{-5}	0.0	5.317×10^{-1}	8.346×10^{-3}	0.0
3.585×10^{4}	-6.992×10^{-5}	0.0	1.137×10^{-2}	-3.226×10^{-1}	0.0
-3.690×10^{3}	1.308×10^{-6}	0.0	3.179×10^{-1}	5.302×10^{-3}	0.0
0.0	0.0	8.407	0.0	0.0	4.849×10^{-2}
0.0	0.0	-6.989	0.0	0.0	-1.956×10^{-3}

K_3 (long-boom controller)

u_{1l}	u_{2l}	u_{3l}	u_{4l}
-3.075×10^{-3}	2.283×10^{-1}	8.108×10^{-1}	2.513×10^{-4}
-5.560×10^{-2}	0.0	0.0	0.0
6.435×10^{-5}	7.019×10^{-4}	1.955×10^{-3}	4.578×10^{-1}
1.592×10^{-4}	0.0	0.0	0.0
-2.265×10^{-4}	5.274×10^{-4}	1.210×10^{-3}	-1.045
-8.686×10^{-4}	0.0	0.0	0.0
7.113×10^{-2}	-1.065	-7.274×10^{-1}	-1.340×10^{-4}
2.447×10^{-1}	0.0	0.0	0.0

K_4 (short-boom controller)

u_{1s}	u_{2s}	u_{3s}	u_{4s}
1.118	-4.244×10^{-4}	-3.878×10^{-3}	5.402×10^{-1}
-1.815×10^{-1}	0.0	0.0	0.0
-1.249×10^{-1}	-5.685×10^{-1}	-4.072×10^{-1}	2.223×10^{-3}
-1.043×10^{-1}	0.0	0.0	0.0
1.521	-8.980×10^{-2}	-4.068×10^{-1}	-5.438×10^{-3}
-2.003×10^{-1}	0.0	0.0	0.0
-6.100×10^{-1}	-5.065×10^{-3}	-3.952×10^{-3}	-1.983×10^{-1}
1.144×10^{-1}	0.0	0.0	0.0

Table 3 Estimator gain constants

K_{1c} (rotational motion estimator)			K_{2c} (translational motion estimator)		
$k_{\theta_{xy}}$	$k_{\theta_{xy}}$	k_{θ_z}	k_{xy}	k_{xy}	k_z
6.217×10^{4}	2.287×10^{-2}	0.0	-2.899×10^{2}	-7.490×10^{-3}	0.0
-9.857×10	-1.508×10^{-2}	0.0	-2.771	2.707×10^{-3}	0.0
1.575×10^{5}	-1.662×10^{-2}	0.0	-1.644×10^{2}	-5.440×10^{-3}	0.0
5.849×10^{2}	1.096×10^{-2}	0.0	-1.932	1.966×10^{-3}	0.0
0.0	0.0	5.648	0.0	0.0	3.183×10^{-2}
0.0	0.0	2.783×10^{2}	0.0	0.0	1.115
2.960×10^{4}	-1.549×10^{-2}	0.0	8.965×10^{2}	2.275×10^{-2}	0.0
4.610×10^{4}	1.371	0.0	1.354×10^{3}	-1.676	0.0
4.457×10^{4}	3.092×10^{-2}	0.0	5.576×10^{2}	1.478×10^{-2}	0.0
-3.079×10^{4}	-2.737	0.0	8.710×10^{2}	-1.089	0.0
0.0	0.0	2.956×10^{2}	0.0	0.0	2.751
0.0	0.0	-1.986×10^{2}	0.0	0.0	-2.202
4.505×10^{5}	-1.124×10^{-4}	0.0	-3.583×10^{2}	-8.450×10^{-3}	0.0
6.702×10^{5}	6.008×10^{-3}	0.0	-2.251×10^{2}	5.143×10^{-1}	0.0
1.725×10^{6}	-6.642×10^{-6}	0.0	-2.645×10^{2}	-5.368×10^{-3}	0.0
2.570×10^{6}	3.551×10^{-4}	0.0	-1.082×10^{2}	3.267×10^{-1}	0.0
0.0	0.0	9.795×10	0.0	0.0	2.369
0.0	0.0	1.308×10^{2}	0.0	0.0	5.966×10^{-1}

K_{3c} (long-boom estimator)			
k_{1l}	k_{2l}	k_{3l}	k_{4l}
4.144×10^{-1}	0.0	0.0	0.0
1.876×10^{-1}	-1.246×10^{-1}	-4.425×10^{-1}	-1.810×10^{-4}
-1.534×10^{-2}	0.0	0.0	0.0
-2.260×10^{-2}	-3.976×10^{-4}	-1.100×10^{-3}	-2.212×10^{-1}
3.520×10^{-2}	0.0	0.0	0.0
6.305×10^{-2}	-2.787×10^{-4}	-6.394×10^{-4}	5.520×10^{-1}
-9.258×10^{-1}	0.0	0.0	0.0
-1.126	5.813×10^{-1}	3.970×10^{-1}	7.468×10^{-5}

K_{4c} (short-boom estimator)			
k_{1s}	k_{2s}	k_{3s}	k_{4s}
9.328×10^{-1}	0.0	0.0	0.0
-5.635×10^{-1}	4.183×10^{-3}	3.824×10^{-3}	-5.325×10^{-1}
5.162×10^{-1}	0.0	0.0	0.0
4.349×10^{-1}	5.604×10^{-1}	4.014×10^{-1}	-2.191×10^{-3}
1.062	0.0	0.0	0.0
-9.076×10^{-1}	8.842×10^{-2}	4.010×10^{-1}	5.361×10^{-3}
-5.624×10^{-1}	0.0	0.0	0.0
2.598×10^{-1}	4.992×10^{-3}	3.895×10^{-3}	1.955×10^{-1}

Conclusions

A design concept for large space structure control systems has been developed in this paper. The approach using pole placement allows the designer to have direct control over the closed-loop system eigenvalues. The numerical problems arising in the pole placement algorithm are examined. With proper frequency scaling and choice of sensor/actuator locations, the numerical difficulties can be removed. This design approach is demonstrated for a representative large space structure. A state estimator controller has also been generated for this system by using the developed computer program.

References

[1] Van Landingham, H.F. and Meirovitch, L., "Digital Control of Spinning Flexible Spacecraft," *Journal of Guidance and Control,* Vol. 1, Sept.-Oct. 1978, pp. 347-351.

[2] Balas, M., "Modal Control of Certain Flexible Systems," *SIAM Journal of Control and Optimization,* May 1978, pp. 450-462.

[3] Likins, P.W., "Dynamics and Control of Flexible Space Vehicles," Jet Propulsion Laboratory, JPL TR32-1329, Jan. 1970.

[4] Tseng, G.T. and Mahn, R.H. Jr., "Flexible Spacecraft Control Design Using Pole Allocation Techniques," *Journal of Guidance and Control,* Vol. 1, July-Aug. 1978, pp. 279-281.

[5] Pistiner, J.S., Tseng, G.T., and Muhlfelder, L., "Multiloop Analysis of a Precision-Pointing Spacecraft with Controlled Flexible Appendages," *Journal of Spacecraft and Rockets,* Vol. 12, Oct. 1975, pp. 586-591.

[6] Skelton, R.E. and Likins, P.W., "An Approach to Model Error Compensation in the Control of Nonrigid Spacecraft," *Proceedings of IFAC, MVTS Symposium,* Fredericton, N.B., Canada, July 1977.

[7] Likins, P.W., Ohkami, Y. and Wong, C., "Appendage Modal Coordinate Truncation Criteria in Hybrid Coordinate Dynamic Analysis," *Journal of Spacecraft and Rockets,* Vol. 13, Oct. 1976, pp. 611-617.

[8] Meirovitch, L., *Analytical Methods in Vibrations,* MacMillan, New York, 1967.

[9] Hurty, W.C., "Dynamic Analysis of Structural System Using Component Modes," *AIAA Journal,* Vol. 3, May 1965, pp. 678-685.

[10] Balas, M., "Feedback Control of Flexible Systems," *IEEE Transactions on Automatic Control,* Vol. AC-23, Aug. 1978, p. 673.

[11] Juang, J.N. and Balas, M., "Dynamics and Control of Large Spinning Spacecraft," *Journal of Astronautical Science,* Vol. XXVIII, No. 1, Jan. 1980, pp. 31-48.

[12] Wu, Y.W., Rice, R.B., and Juang, J.N., "Sensor and Actuator Placement for Large Flexible Space Structures," *Proceedings of Joint Automatic Control Conference,* Denver, Colo., June 1979, p. 230.

[13] Simon, J. and Mitter, S., "A Theory of Model Control," *Information and Control,* Vol. 13, 1968, p. 316.

[14] Gould, L., Murphy, A., and Berkman, E., "On the Simon-Mitter Pole Placement Algorithm," *IEEE Transactions on Automatic Control,* Vol. AC-15, 1970, p. 259.

[15] Wonham, W.M., "On Pole Assignment in Multi-Input Controllable Linear Systems," *IEEE Transactions on Automatic Control,* Vol. AC-12, 1967, p. 660.

[16] Chen, C.T., *Introduction to Linear System Theory,* Holt, Rhinehart and Winston, Inc., New York, 1970.

[17] Bryson, A.E. Jr. and Ho, Y.C., *Applied Optimal Control,* Blaisdell Publishing Co., Waltham, Mass., 1969.

[18] Anderson, B.D.O. and Moore, J.B., *Linear Optimal Control,* Prentice-Hall, Englewood Cliffs, N.J., 1971.